DIPLOMA THESIS

Metabolism in lung cancer: *Ex vivo* analysis with stabile isotope labelled tracers

submitted by

Julia Michaela Lesko

for the academic degree of

Doktor(in) der gesamten Heilkunde

(Dr. med. univ.)

at the

Medical University of Graz

Department of Internal Medicine

Division of Pulmonology

under supervision of

Univ.-Ass. Priv.-Doz. Dr. med. univ. Katharina Leithner, PhD

and

Assoz. Prof. Priv.-Doz. Dr. rer. nat. Andelko Hrzenjak

Graz, 27th April 2018

Statutory declaration

I declare that I have authored this diploma thesis independently, that I have not used other than the declared sources, and that I have explicitly marked all material which has been quoted either literally or by content from the used sources.

Graz, 27th April 2018 *Julia Lesko, eh*

Acknowledgement

For her supervision and excellent assistance, I would like to thank my supervisor Univ.-Ass. Priv.-Doz. Dr. med. univ. Katharina Leithner, PhD.

Many thanks to Assoz. Prof. Priv.-Doz. Dr. rer. nat. Andelko Hrzenjak for his co-supervision and helpful support. Great thanks to Alexandra Bertsch, M.Sc. for her help to incorporate me into labour work, especially to produce histological slides.

I would also like to thank Alexander Triebl, PhD Core Facility Mass Spectrometry and Lipidomics at the Center for Medical Research (CMR, ZMF), Medical University of Graz, for performing mass spectrometry analyses and detailed explanations. I am grateful for the support by PD. Dr. med. univ. Elvira Stacher-Priehse, Institute of Pathology at the Medical University of Graz.

I appreciated to get the possibility to work in the research group of Prof. Dr. Horst Olschewski at the Division of Pulmonology, Department of Internal Medicine at the Medical University of Graz.

Finally, I thank my family and Florentin for their support during my medical studies.

Table of contents

Abbreviations

α-KG	α-ketoglutarate
ATP	adenosine triphosphate
DHAP	dihydroxyacetone phosphate
DMEM	Dulbecco's modified Eagle´s media
G3P	glycerol 3-phosphate
GLS	glutaminase
HE	haematoxylin and eosin
HIF1	hypoxia-inducible factor 1
LC	liquid chromatography
MS	mass spectrometry
MTBE	methyl-*tert*-butyl-ether
m/z	mass-to-charge
NSCLC	non-small cell lung cancer
OAA	oxaloacetate
OD	optical density
PBS	phosphate buffered saline
PC	phosphatidylcholine
PCK2	phosphoenolpyruvate carboxykinase 2
PE	phosphatidylethanolamine
PEP	phosphoenolpyruvate
PEPCK	phosphoenolpyruvate carboxykinase
PI	phosphatidylinositol
SCLC	small cell lung cancer
TCA	tricarboxylic acid
WHO	World Health Organisation

List of figures

List of tables

Abstract (German)

Der Metabolismus von Tumorzellen ist an die rasche Zellteilung angepasst. Eine erhöhte Synthese von Lipiden, insbesondere die Synthese von Phospholipiden als Baustein von Zellmembranen, ist wichtig für die Zellproliferation. Daher werden metabolische Stoffwechselwege als mögliche therapeutische Angriffspunkte zur Behandlung von Krebserkrankungen intensiv untersucht, diese werden jedoch stark von der tumorspezifischen Mikroumgebung *in vivo* beeinflusst. Untersuchungen an Gewebemodellen *ex vivo* können neue Erkenntnisse liefern.

Das Ziel dieser Studie war, ein *ex vivo* Modell zu etablieren, welches die Untersuchung der Phospholipidsynthese in Lungenkrebszellen unter physiologischen Bedingungen ermöglicht. Es wurden Gewebefragmente aus frischem Lungengewebe sowie präoperativ unbehandelten Lungentumoren (Nicht-kleinzelliges Lungenkarzinom) von sieben PatientInnen für 72 Stunden kultiviert. In diesen Fragmenten wurde in Tracerversuchen die Konversion von $^{13}C_6$-Glukose und $^{13}C_5$-Glutamin zu phospholipidgebundenem Glycerin untersucht. Glukose liefert das Glycerinrückgrat der Phospholipide dabei über den Stoffwechselweg der Glykolyse, während Glutamin potenziell entlang des Glyceroneogeneseweges zu Glycerinphosphat umgewandelt werden kann. Die Konzentration der isotop markierten Glukose in den Medien entsprach entweder physiologischen (5 mM) oder nährstoffarmen, tumorspezifischen Bedingungen (1 mM). Die Aufnahme markierter Kohlenstoffatome ins Glycerin der Phospholipide wurde mit Hilfe von Flüssigchromatographie und Massenspektrometrie analysiert.

Die zu mehreren Zeitpunkten gemessene Vitalität der Fragmente war variabel. Jedoch war in allen Proben im gesamten Verlauf des Experiments vitales Gewebe vorhanden. Tumorfragmente zeigten nach 72 Stunden mehr nekrotische Veränderungen im Vergleich zu Lungenfragmenten.

Der Einbau von $^{13}C_6$-Glukose ins phospholipidgebundene Glycerin (es resultiert ein Glycerinfragment mit drei ^{13}C) wurde sowohl in Tumor- als auch Lungenfragmenten entdeckt. Interessanterweise war der Anteil des Einbaus bei Lunge und Tumor ähnlich. Die Kontrollgruppe mit unmarkierter Glucose zeigte keine Anreicherung. Unabhängig vom Nährstoffgehalt wurde $^{13}C_5$-Glutamin nicht zu Glycerin konvertiert. Dieses *ex vivo* Modell eignet sich gut zum Nachweis der Konversion von $^{13}C_6$- Glukose in das phospholipidgebundene Glycerin in frischen Lungen- und Tumorfragmenten. Aufgrund des Gebrauchs von PatientInnengeweben in einem

dreidimensionalen Kontext unter (patho-)physiologischen Bedingungen, erlaubt dieses Modell die Untersuchung des Tumormetabolismus unter Bedingungen, die der *in vivo* Situation ähnlich sind. Ein limitierender Faktor ist die beeinträchtige Gewebevitalität aufgrund der *ex vivo* Kultivierung. Kürzere Inkubationszeiten und verbesserte Kulturbedingungen (schütteln oder schaukeln, etc.) könnten die Vitalität der Fragmente erhöhen.

Abstract

The metabolism of tumour cells is adapted to rapid cell division. Increased lipid synthesis, particularly of phospholipids as component of cell membranes, is crucial for cell proliferation. Thus, metabolic pathways are intensively studied as potential therapeutic approach for cancer treatment, however they are highly influenced by tumour-specific microenvironment *in vivo*. Research in *ex vivo* tissue models may provide new findings.

The aim of this study was to establish an *ex vivo* model that allows to investigate phospholipid synthesis in lung cancer cells under physiological conditions. Tissue fragments from fresh lung and preoperative untreated non-small cell lung cancer (NSCLC) of seven patients were cultured for 72 hours. In tracer experiments using these samples, we analysed the conversion of $^{13}C_6$ glucose and $^{13}C_5$ glutamine into the glycerol moiety of phospholipids. Glucose provides the glycerol-backbone of phospholipids via glycolysis, while glutamine is potentially metabolised to glycerol-phosphate via glyceroneogenesis. The concentration of $^{13}C_6$ glucose in the media corresponded to physiological (5 mM) or nutrient-poor, tumour-specific (1 mM) conditions. Incorporation of labelled carbons into the glycerol moiety was analysed by liquid chromatography and mass spectrometry.

Fragment viability, measured after several time intervals, was variable. However, viable tissue was present in all samples during the entire experimental course. Tumour fragments showed more necrotic changes compared with lung fragments after 72 hours. An incorporation of $^{13}C_6$ glucose into the phospholipid-linked glycerol (yielding a glycerol-fragment with three ^{13}C) was detected both in tumour and lung fragments. Interestingly, the rate of incorporation into lung or tumour tissue was similar. The control group with unlabelled glucose did not show any enrichment. Independent of the nutrient content, $^{13}C_5$ glutamine was not converted into the glycerol moiety.

This *ex vivo* model is well suited for studying the conversion of $^{13}C_6$ glucose into the glycerol backbone of phospholipids in fresh lung and tumour fragments. By using patient-derived tissue in its three-dimensional context in patho-/physiological nutrient conditions, this model enables investigating tumour metabolism under conditions mimicking the situation *in vivo*. As a limitation, *ex vivo* culture impairs tissue viability. Shorter incubation time and improved culture conditions (shaking or rocking, etc.) might enhance fragment viability.

1 Introduction

1.1 Lung Cancer

1.1.1 Epidemiology

The World Health Organisation (WHO) World cancer report 2014 shows that estimated 14.1 million new cases of cancer were diagnosed and 8.2 million affected persons died because of cancer in 2012. Lung cancer had among men the highest estimated incidence with 16.7%, followed by prostate cancer (15.0%), and highest estimated mortality rate with 23.6% worldwide in 2012. Among women, it was estimated, that the incidence of breast cancer ranked first (25.2%), followed by colorectal carcinoma (9.2%) and lung cancer with 8.7%. With a mortality of 13.8% lung cancer counted the second most common cause in cancer death behind breast cancer (14.7%). Combining data for both sexes, lung cancer was the most diagnosed cancer disease worldwide (13.0% of the total) (1).

In Austria's population lung cancer accounts for the most frequent malignancies. Table 1 shows the trend of mortality and incidence age-standardized rates (per 100.000 persons/men/women, European standard population, 2013) between 1984 and 2014. In this time, incidence rate increased from 21.1 to 40.4 per 100.000 women and mortality rate increased from 20.5 to 32.0 per 100.000 women. In opposite, both incidence rate and mortality rate decreased among men in this time. With growing number of new cases of lung cancer, the mortality rate among women increased despite advanced therapies in recent years. Overall, between 1984 and 2014 the incidence rate decreased slightly from 59.6 to 56.9 and mortality rate from 56.1 to 47.3 cases per 100.000 persons (2, 3).

Table 1 | **Incidence and mortality age-standardized rates of lung cancer in Austria**

	Incidence rate				**Mortality rate**			
Year	**1984**	**1994**	**2004**	**2014**	**1984**	**1994**	**2004**	**2014**
Women	21.1	25.7	33.3	40.4	20.5	23.0	26.2	32.0
Men	124.5	104.3	90.5	78.7	117.4	97.1	79.1	68.0
Total	59.6	56.1	57.1	56.9	56.1	51.2	48.0	47.3

Data by STATISTIK AUSTRIA, Austrian carcinoma register (version 28.11.2016) from (2, 3). In each case age-standardized rates per 100.000 persons/men/women are shown, European standard population, 2013.

1.1.2 Aetiology

Tobacco smoking, including second-hand smoke, is the major risk factor for lung cancer. Duration and amount of exposure to tobacco smoke ("pack-years") impact the risk to develop lung carcinoma. Furthermore, thoracic and respirable particle with a diameter less than 10 µm, including also asbestos fibres, are carcinogenic. Arsenic, radon and air pollution are also recognized to cause lung cancer. Workers in certain departments, such as dye industry or rubber industry, have an increased risk for lung cancer (1, 4).

1.1.3 Classification

The 2015 WHO Classification indexes lung cancer based on their morphology, histology, and immunohistochemistry (5, 6). Lung cancer is divided in two major categories: non-small cell lung cancer (NSCLC) and small cell lung cancer (SCLC). Epithelial tumours as adenocarcinoma, squamous cell carcinoma, large cell carcinoma, and sarcomatoid carcinoma with subtypes are summarised as NSCLC and account for 85% of lung cancer (5, 7, 8). The second largest group are SCLC at around 15% (9).

1.1.4 Staging

The TNM staging system is used internationally to define different severities of a tumour. It is based on three descriptors: the regional extent of the tumour (size and depth of infiltration) (T), regional lymph node involvement (N), and the existence of metastasis (M) (Table 2). The TNM stage plays the most important role for the choice of a treatment and the prognosis for survival. Furthermore, it provides information about the success of an applied treatment for clinical research. The advantages of this classification are the universal and reproducible applicability (10, 11). The tumours included in our study were classified according to 7th lung cancer TNM classification, however since January 1st 2017 the novel 8th version is in use (10, 12). It includes several changes: T descriptors for lung cancer were changed. Now, every T stage is defined by new size cut points so that the importance of tumour size for prognosis is considered (13, 14). The division of existing remote metastasis were adapted. The N category of the 7th version was reviewed and maintained the same (13).

Table 2 | **Staging according to the 7th lung cancer TNM classification 2009**

Stage	T	N	M
Occult Carcinoma	Tx	N0	M0
0	Tis	N0	M0
IA	T1a - T1b	N0	M0
IB	T2a	N0	M0
IIA	T2b	N0	M0
	T1a/b -T2a	N1	M0
IIB	T2b	N1	M0
	T3	N0	M0
IIIA	T1 – T3	N2	M0
	T3	N1	M0
	T4	N0 - N1	M0
IIIB	T1 - T4	N3	M0
	T4	N2	M0
IV	Any T	Any N	M1a - M1b

Abbreviations: T, primary tumour; N, regional lymph node; M, distant metastasis; Tx, primary tumour cannot be assessed; Tis, carcinoma *in situ*. Adapted from Lababede (10).

1.2 Tumour metabolism

1.2.1 Metabolic reprogramming in cancer

Tumour tissue is composed of neoplastic, autonomous cells and normal supplemental cells, whose interactions and metabolism influence the tumour microenvironment. Non-transformed cells, such as involved immune cells, vasculature components, fibroblasts and other cells, work together in a highly complex tumour network (15, 16). In order to support survival and proliferation, cancer cell metabolic pathways are rewired by oncogenic signalling pathways (17-19). Abnormal cells pursue three aims to drive growth: energetics – generation of energy in the form of adenosine triphosphate (ATP), biosynthesis – building of required macromolecules, and cellular homeostasis – maintenance of an optimal cellular redox status (18).

1.2.2 The role of glutamine and glucose

Glucose and glutamine belong to the most abundant nutrients in mammalian cells and are essential for carbon and nitrogen metabolism (20, 21). Cancer cells modify their metabolism by preferentially using glucose and glutamine to secure the

demand of carbons and free energy (22, 23). Oncogenes, such as MYC or Ras, regulate the use of these important carbon sources for metabolic pathway in order to ensure tumour growth (24).

1.2.3 The metabolic cancer microenvironment and hypoxia

The tumour's microenvironment differs from normal tissues in many aspects. Especially, the supply of crucial nutrients as glucose, glutamine, and oxygen is temporally heterogeneous (17, 18, 25). Tumour cells must stimulate angiogenesis, the growth of new blood vessels, to be able to grow. However, the novel vascular network is often discontinuous, abnormal, and blood vessels are leaky (23, 26). With increasing distance to vessels cancer cells show a demand of nutrients as well as oxygen and are disadvantaged in using their preferred metabolic pathway (24). Therefore, despite the process of vascularisation, cancer cells are often compelled to proliferate in a hypoxic, acidotic, and nutrient-poor setting (17, 23, 25). Cancer cell metabolism plays a special role in the generation of building blocks that are required for cell division. Although the preferred tricarboxylic acid (TCA) cycle (the Krebs cycle) supplies by mitochondrial oxidative phosphorylation up to 38 ATP molecules per each molecule glucose, tumour cells switch their way to get energy. They use anaerobic glycolysis that provides only two ATP per molecule of glucose by generating lactate (22, 25). Tumour cells frequently choose aerobic glycolysis for energy generation, irrespective of oxygen concentrations. This phenomenon is referred to as "Warburg effect" after Otto H. Warburg (22, 27). Although the profit of ATP from glucose is low, upregulation of aerobic glycolysis during carcinogenesis leads to a growth advantage for neoplastic cells, since glycolysis provides metabolic intermediates for diverse important biosynthetic pathways (28). In addition, it enables cancer cells to proliferate in a hypoxic milieu. Thus, the "Warburg effect" facilitates tumour growth and it is directly enhanced by oncogenes. However, the TCA cycle is still functional in cancer cells. It provides precursors for anabolic biosynthesis, e.g. of amino acids (20, 29, 30).

1.3 Glucose as carbon source

The importance of glucose for tumours is highlighted by the upregulation of aerobic glycolysis, the "Warburg effect" (31, 32). Increased aerobic glycolysis in cancer cells provides carbons for many anabolic reactions and subsequently, a selection benefit for the tumour cells in an unfavourable microenvironment with prevailing acidosis

and hypoxia (28). Intermediates of the glycolytic pathway are used to generate a major part of products for many cell functions and especially for cancer cell proliferation (28, 31). Transcription regulators, such as hypoxia-inducible factor 1 (HIF1) and MYC oncogene, are highly activated in cancer and play an important role for an increased expression of glucose transporters and glycolytic enzymes (15, 33). The three major biosynthetic pathways fuelled by glycolysis are the biosynthesis of ribose phosphate for the generation of deoxyribonucleic acid, the biosynthesis of glycerol phosphate for the biosynthesis of glycerol-containing lipids, and the biosynthesis of serine (32, 34). In our study we focused on the synthesis of glycerol phosphate from glucose, since lipids, especially phospholipids, are important constituents of cell membranes (23, 35).

1.4 Glutamine as carbon source

Recent studies exhibited that glutamine plays an important role as a nitrogen donor required in the synthesis of nucleotides or certain amino acids, as well as a carbon source for diverse biosynthetic pathways and to support homeostasis (20, 24). Cancer cells show both a higher glutamine uptake and increased activity of the enzyme glutaminase (GLS) (36). MYC affects, via transcriptional upregulation of glutamine transporters and glutamine-related enzymes (e.g. glutaminase-1), the glutamine metabolism of cancer cells, too (15).

Glutamine is channelled through transporters into mitochondrion, enters the TCA cycle via alpha-ketoglutarate (α-KG) and is converted to oxaloacetate (OAA) (37). The enzyme phosphoenolpyruvate carboxykinase (PEPCK) metabolises OAA to phosphoenolpyruvate (PEP) (19, 38). Physiologically this enzyme plays an important role in the synthesis of glucose (gluconeogenesis), as well as glycerol (glyceroneogenesis) and the conversion of amino acids, such as glutamine, to PEP (38, 39). PEP leaves the mitochondrion and is metabolised along the gluconeogenesis pathway, which correlates with the glyceroneogenesis pathway up to the intermediate dihydroxyacetone phosphate (DHAP) (34). Because of the limited amount of published data, Leithner et al. investigated the function of the mitochondrial isoform of PEPCK, phosphoenolpyruvate carboxykinase 2 (PCK2), in lung cancer. PCK2 showed in three lung cancer cell lines an increased activity to catalyse the reaction from OAA to PEP under low glucose conditions (39). An enhanced expression and activity of PEPCK (PCK1 or PCK2) in cancers has been

described also by other groups in the recent years (19, 40). In gluconeogenic organs, e.g. in liver, brain, and skeletal tissue, cells utilize the gluconeogenic pathway to generate glucose from non-carbohydrate precursors such as lactate and amino acids. In addition, the liver covers its demand for glycerol 3-phosphate (G3P) by glyceroneogenesis (34).

1.5 Synthesis of phosphoglycerides

Cancer cells show an increased requirement for lipids (23). Lipids play a central role as constituents of cell membranes; they are incorporated into lipid droplets or used as signalling lipids (23, 41). On one hand, glucose and glutamine provide most of the carbon to generate new lipids; on the other hand, lipids are retrieved from exogenous sources (22). Phospholipids occur as lipid bilayers in great quantities in all biological membranes (34, 41). They divide not only cell compartments from each other, but also transmit intracellular signals and are important for cell division, cell movement, and other purposes (41). Phospholipids containing glycerol are so-called phosphoglycerides or glycerophospholipids. They are composed of four moieties: glycerol, phosphate, alcohol, and one or more fatty acids as shown in Figure 1 (34, 41).

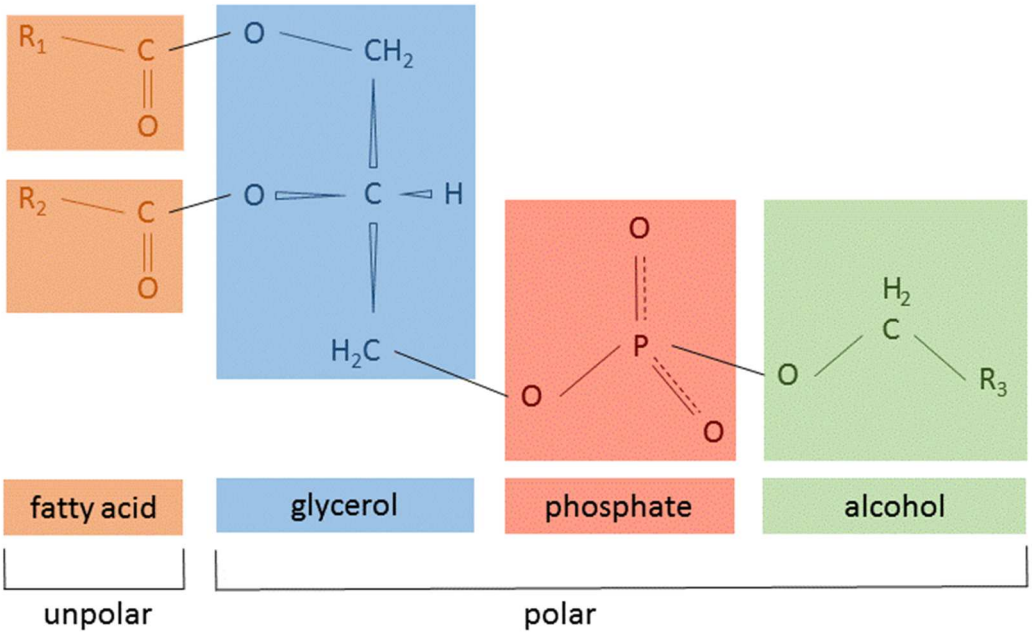

Figure 1 | **Structure of phosphoglycerides.** Phospholipids consist of a hydrophilic (polar) as well as lipophilic (unpolar) part. Thus, they have important physical amphipathic properties. The polar head group is composed of phosphate esterified on one side with an alcohol; and, on the other side with the hydroxyl group at C-3 (carbon at the third position) of glycerol. The hydroxyl group at the first and second carbon positions of glycerol are esterified with a saturated or an unsaturated fatty acid. The hydrophobic part of phospholipids is built by the long chain fatty acids.

In mammalian cells, phosphoglycerides are generated *de novo*, recycled from cell membranes, or derived from triglycerides. Dividing cells show an increased synthesis of phosphoglycerides (35). In mammalian cells the first step in phosphoglyceride synthesis is the generation of phosphatidate (diacyglycerol 3-phosphate). Phosphatidate is synthesized both in the endoplasmatic reticulum and the outer mitochondrial membrane. The reduction of DHAP results in G3P, which forms the starting point of this pathway. G3P reacts directly with two activated fatty acids (usually one saturated and one unsaturated) to phosphatidate, catalysed by the enzyme glycerol phosphate acyltransferase (34). The next step is catalysed either at the endoplasmatic reticulum or at the Golgi apparatus: the esterification reaction between the phosphate group of phophatidate and the hydroxyl group of an alcohol. This anabolic step takes place via activating one of the components. Activation of the head group results in generating phosphatidylethanolamine (PE) and phosphatidylcholine (PC). Phosphatidylinositol (PI) is built by activation of the glycerol unit (34).

1.6 *Ex vivo* cancer models ("organoid models")

Cell culture studies are suitable to examine cell-specific pathways; however, they are unable to provide information about processes in tissue. Thus, in the past years increasingly *ex vivo* tissue models have been used, that mimic the tissue architecture *in vivo* ("organoid models") under near-physiological conditions. In contrast to cell lines, organoids are composed of diverse cell types including stroma cells (42). Tumour proliferation is modulated by cell-cell-interactions and signalling by stroma cells, such as fibroblasts and endothelial cells (tumour microenvironment). Cancer cells use functions of normal cells for cancer growth (43). Research with organoids allows investigating cancer metabolism in the complex 3D context and microenvironment of tumours (42). This approach is frequently also used for stem-cell research or for the study of drug effects (44). *Ex vivo* models with fresh tissue fragments, treated and incubated for a few days, should give us an insight into the metabolic pathways of cells influenced by their microenvironment (45).

1.7 ^{13}C metabolite labelling in cancer research

The use of stable isotope labelled tracers offers a comprehension, how metabolites are converted along a known pathway (35, 46). Detection of ^{13}C labelled “heavy” metabolites with MS has the advantage to measure selectively and concurrently chosen labelled atoms in a mix of metabolites (35). MS is the preferred procedure in lipidomic research (47). In our study, stable isotope analysis was used to assess the flux from glucose and glutamine to glycerol in lung cancer tumour fragments, under starvation and non-starvation conditions.

1.7.1 Analytic procedures: chromatography and mass spectrometry

Chromatography combined with MS is one of the best applicable techniques in the important field of cancer metabolism and lipid research (47). Chromatography is a laboratory technique used to separate mixtures into their components. The procedure is based on a stationary phase (e.g. solid), which is flowed through by a mobile phase (gas or liquid) containing the mixture. The separation happens by their interaction with the stationary phase in a chromatography column, which occurs at different rates. Compounds with a higher affinity to the stationary phase migrate more slowly than compounds that tend toward the mobile phase. Equal compounds reach a detector at the same time and these signals are shown as a peak in a chromatogram (48).

2 Hypothesis and aims of the study

Most research in the field of cancer metabolism, and specifically cancer lipid metabolism, is performed on cancer cell lines or animal models, which might not reflect the actual situation in human lung cancers *in vivo*. To assess lipid synthesis in human cancer cells *in vivo*, it would require continuous infusion of stable isotope tracers, which is not feasible in most laboratories. On the other hand, the impact of systemic metabolic reactions (e.g. in the liver) is enormous and cannot be separated from the tumour metabolism. Therefore**,** it needs models, allowing the analysis of lipid synthesis pathways in human cancer, mimicking the natural microenvironment.

The aim of the study was to assess the feasibility and limitations of the use of stable isotope tracers, combined with MS-based analysis of phospholipids in fresh human lung and lung cancer, cultured *ex vivo*. Seven patients with diagnosed NSCLC were included in this pilot study. Nutrient-rich and nutrient-poor conditions were analysed.

The second aim of this pilot study was to analyse the metabolism of $^{13}C_6$ labelled glucose via glycolysis as well as the metabolism of $^{13}C_5$ labelled glutamine along the glyceroneogenesis pathway in fresh NSCLC tissue fragments. The target variable was the percentage of stable isotope labelled carbon-skeleton of glycerol incorporated into to phospholipids after incubation with $^{13}C_6$ labelled glucose or $^{13}C_5$ labelled glutamine under starvation and non-starvation conditions. As a control, the same proportion was analysed in tissue fragments incubated with unlabelled glucose or glutamine.

My personal intent of this diploma thesis was to gain insight into the laboratory work and basic medical research.

3 Material and methods

3.1 Patients

This pilot study included seven patients with following recruitment criteria: patients with primary NSCLC devoid of neoadjuvant chemotherapy. NSCLC samples and corresponding normal lung tissue samples were received from patients, who were referred for surgical resection (lobectomy) to the Division of Thoracic and Hyperbaric Surgery at the Medical University of Graz in cooperation with Assoz. Prof. Priv.-Doz. Dr. Jörg Lindenmann, from January to May 2016. The study protocol was approved by the ethics review board of the Medical University of Graz. Signed informed consent was obtained from all patients prior to surgery.

3.2 *Ex vivo* culture of normal and lung cancer fragments

After lobectomy, tissues were transported to the Institute of Pathology at the Medical University of Graz, for frozen-section diagnosis. Immediately after arrival, fresh lung and tumour tissue samples were inserted into cold phosphate buffered saline (PBS) pH 7.4 (pharmacy, State Hospital Graz, Austria) and, as fast as possible, further processed for culture (average time from surgical removal to culture: 2 hours 39 minutes). Using a razor blade, the tumour and lung tissues were fractionated in equal fragments with around 1-2 mm diameter. For the lung and the tumour samples, three six-well plates for each condition were made. Up to six fragments were transferred into one well. Each well was filled with 2 ml of growth medium. The tissue fragments were incubated in a CO_2-incubator under standard oxygen conditions at 37°C for 72 hours.

3.2.1 Growth media

Non-starvation and starvation media were used, for both, lung and tumour fragments (Table 3 and 4). Media contained either uniformly ^{13}C-labelled glucose, uniformly ^{13}C-labelled glutamine, or no tracer. To ensure constant conditions, 1.9 ml of the medium in each well were changed every 24 hours.

Non-starvation conditions

For non-starvation treatment, Dulbecco's modified Eagle´s media (DMEM) (Gibco, Carlsbad, CA, USA) without glucose and glutamine, supplemented with 10% dialyzed fetal bovine serum (Gibco), 100 U/ml penicillin (Gibco), and 100 µg/ml streptomycin (Gibco) was used. Unlabelled glucose (Gibco) or uniformly labelled

glucose ($^{13}C_6$ glucose) (Cambridge Isotope Laboratories, Tewksbury, MA USA), as well as unlabelled glutamine (Gibco) or $^{13}C_5$ glutamine (Sigma-Aldrich, St. Louis, MO, USA) were added as described in Table 3. Stocks of labelled or unlabelled glucose or glutamine were diluted in Aqua dest., sterile filtered through 0.22 µm filters and stored at -20°C. The used composition corresponds to physiological, non-starving conditions *in vivo*.

Table 3 | **Composition of media for non-starvation**

Medium	Glucose	Glutamine	$^{13}C_5$ glutamine	$^{13}C_6$ glucose	Dialyzed serum
1	5 mM	1 mM	-	-	10%
2	5 mM	-	1 mM	-	10%
3	-	1 mM	-	5 mM	10%

Starvation conditions

For treatment under starvation conditions, the specimens were cultured in DMEM glucose-glutamine-free medium (Gibco) containing 0% dialyzed fetal bovine serum (Gibco), as well as 100 U/ml penicillin (Gibco) and 100 µg/ml streptomycin (Gibco). Unlabelled glucose (Gibco) or $^{13}C_6$ glucose (Cambridge Isotope Laboratories), as well as unlabelled glutamine (Gibco) or $^{13}C_5$ glutamine (Sigma-Aldrich) were added as described in Table 4. Stocks of labelled or unlabelled glucose or glutamine diluted in Aqua dest. and sterile filtered through 0.22 µm filters were stored at -20°C.

Table 4 | **Composition of media for starvation**

Medium	Glucose	Glutamine	$^{13}C_5$ glutamine	$^{13}C_6$ glucose	Dialyzed serum
1	1 mM	1 mM	-	-	0%
2	1 mM	-	1 mM	-	0%
3	-	1 mM	-	1 mM	0%

3.3 Measurement of fragment size

After 72 hours of incubation, the size of tumour and lung fragments were measured using the inverted microscope Olympus Basic IX51 (OLYMPUS, Shinjuku, Tokio, Japan). At 100-fold magnification, maximum and minimum diameters of each fragment were determined with CellSens Standard 1.8.1. software (OLYMPUS). From two patients, 30 lung and 30 tumour fragments cultured under non-starvation conditions were measured. From the third patient, 16 lung and 16 tumour fragments cultured under starvation conditions were measured.

3.4 MTS assay

The MTS Cell Proliferation Colometric Assay Kit (Biovision, Milpitas, CA, USA) was conducted to assess the viability of tumour and lung fragments at 0, 24, 48 and 72 hours after the beginning of the treatment. This method is based on the reduction of MTS tetrazolium caused by viable cells. A coloured formazan is created by this reaction. The assay was performed according to the manufacturer´s protocol. 20 µl MTS reagent (Biovision) was added to culture media, supplemented with 10% dialyzed fetal bovine serum (Gibco) and antibiotics (Gibco), not containing phenol red. Fragments were incubated in MTS-containing medium in 96-well plates (one fragment/well) for three hours. Then, fragments were transferred with a tweezer in PBS. After dabbing the fragments, the weight of each was measured. The optical density (OD) of the formazan in the medium was analysed by a spectrophotometer SPECTRAmax PLUS 384 (Molecular Devices, Sunnyvale, CA, USA) with SoftMax Pro Software (Molecular Devices) at 490 nm. Tumour and lung fragments treated 30 minutes in 70% ethanol were used as a control. OD values were normalized to the weight of each fragment.

3.5 Fixation and histological processing of tumour and lung tissues

Fresh lung and tumour tissues, as well as lung and tumour fragments, were fixed after 72 hours of treatment in unlabelled medium in buffered 4% formaldehyde solution (pharmacy, State Hospital Graz, Austria) for at least 24 hours. The fixed tissues were transferred into embedding cassettes for paraffin wax fixation. The Tissue-Tek VIP (Sakura, Staufen, Germany) dehydrates the tissues through a series of graded ethanol baths, and then infiltrated them with paraffin wax. In the next step, the tissues were embedded in paraffin blocks. When the wax was completely hardened, the tissues were sectioned using a microtome MICROM HM 355S (Thermo Fisher Scientific Inc., Waltham, MA, USA). At the end, 2 µm section were stained with haematoxylin and eosin (HE stain).

3.6 Microscopic evaluation of viability

Morphological appearance and viability were analysed using HE stained sections, together with the thoracic pathologist PD Dr. Elvira Stacher-Priehse. Pictures were taken with the inverted microscopy system Olympus Basic IX51 (OLYMPUS).

3.7 Stable isotope tracer experiments in *ex vivo* tissue fragments and analysis by mass spectrometry

Conversion of $^{13}C_6$ labelled glucose and $^{13}C_5$ labelled glutamine to glycerol attached at PC, PE and PI was measured using liquid chromatography (LC) and mass spectrometry (MS). The LC-MS analysis was performed by Alexander Triebl, PhD Core Facility Mass Spectrometry and Lipidomics (CMR), Medical University of Graz.

3.7.1 Sample preparation

After 72 hours of incubation at 37°C under ambient oxygen conditions, the tissue fragments were prepared for MS. First, each fragment group was collected using a tweezer and washed in DMEM glucose-glutamine-free medium (Gibco). Afterwards, the samples were transferred to 1.5 ml ice-cold methanol (Merck, Darmstadt, Germany). Samples were homogenised using an Ultraturrax until a sufficiently homogeneous suspension was reached, followed by sonication three times for 10 seconds on ice. The homogenate was transferred in precooled glass Pyrex tubes. These tubes were stored at -20°C until MS analysis. Methyl-*tert*-butyl-ether (MTBE) extraction of lipids was performed by Alexander Triebl, PhD Core Facility Mass spectrometry and Lipidomics (CMR), Medical University of Graz, as described (49).

3.7.2 Chromatography and mass spectrometry

Chromatography and MS were performed by Alexander Triebl, PhD Core Facility Mass Spectrometry and Lipidomics (CMR), Medical University of Graz. Initially, a high-performance LC modified after Triebl et al. (50) was performed using a Phenomenex Kinetex HILIC column (2.1 mm x 100 mm, 2.6 µm) (Phenomenex, Aschaffenburg, Germany). For determination of the phospholipid head group fragment ions of PC, PE, and PI, either with, or without glycerol, the Orbitrap Velos Pro mass spectrometer (Thermo Fisher Scientific Inc.) was used (49).

MS is used to detect metabolites according to their mass-to-charge ratio (*m/z*). This technique involves three steps: ionisation of organic and inorganic substances, sorting of the generated ions according to their *m/z* and qualitative and quantitative detection. In consequence of ionization, the molecular structure of the substances is changed. Figure 2 shows the graphic representation of the results, a mass spectrum (51).

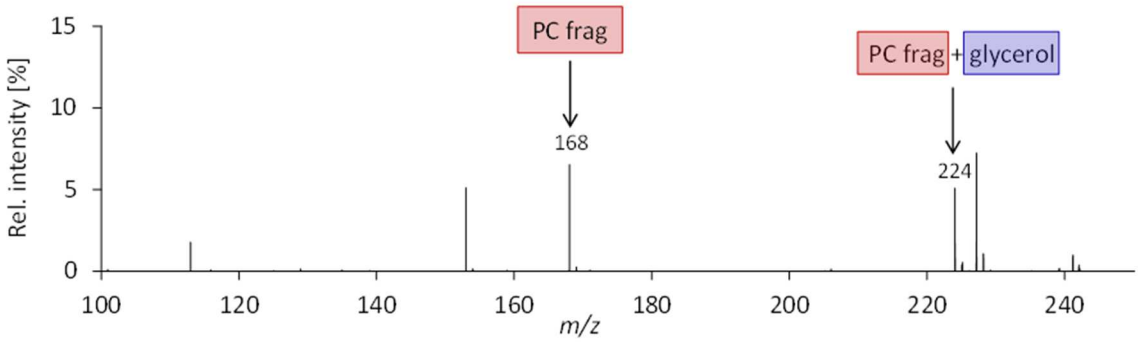

Figure 2 | **Mass spectrum of PC fragments with or without glycerol.** The mass spectrum showing signal intensities on the y-axis and the mass-to-charge ratio (*m/z*) on the x-axis. The phosphatidylcholine head group fragment ion not containing glycerol (PC frag) has a *m/z* of 168, while the fragment containing glycerol (PC frag + glycerol) has *m/z* of 224. MS was performed by Alexander Triebl, PhD Core Facility Mass Spectrometry and Lipidomics (CMR), Medical University of Graz. With permission from Alexander Triebl, PhD (49).

Isotopes are elements with an equal number of protons, but a different quantity of neutrons in the atomic nucleus (consequentially, a different atomic mass, thus a different mass number) (52). Calvert defined: isotope pattern in MS as a ”Set of peaks related to ions with the same chemical formula but containing different isotopes.” (53). Molecules that vary only in their quantity of isotopic substitutions are referred to as “isotopologues” (54).

Carbon (^{12}C) has naturally occurring isotopes, ^{13}C and ^{14}C (55). The rate of ^{13}C must be considered, when stable isotope enrichment in ^{13}C labelling experiments is evaluated. In a mass spectrum without isotope labelled tracers, the M+1 peak (the first isotopic peak) corresponds with the natural abundance. For each fragment head group, the peaks of the respective isotopologues were normalised to the peak of the monoisotopic isotopologues (49). The mass spectrometric data were corrected for natural abundance of ^{13}C, using control samples grown in media 1 and 4 containing unlabelled glucose or glutamine. This correction is necessary since 1.1% of naturally occurring carbons are ^{13}C isotopes. Table 5 illustrates the natural abundance of carbon isotopes (55).

Table 5 | **Natural abundance of carbon isotopes**

C isotopes	Atomic mass [u]	Natural abundance
^{12}C	12	98,89%
^{13}C	13	1,11%

3.8 Statistical analysis

Statistical analysis was calculated using SPSS software (version 23) and Microsoft Excel (2016). Results are shown as mean ± SEM (from n = 3 or 4 patients per each group). Groups were compared using Student's t-test, Mann-Whitney-U-Test and One-Way ANOVA with Tukey´s HSD Post hoc test. The level of statistical significance was defined as $p < 0.05$.

4 Results

4.1 Clinical information

All clinical data were retrieved by the clinical data system of the State Hospital and Medical University of Graz, Austria. Seven patients (3:4 male to female ratio) with NSCLC-stages IA to IIIA were included. The median age was 67 years (range 54 years to 83 years). Patient and tumour specific data are listed in Table 6.

Table 6 | **Patients' clinical data**

Patient	#1	#2	#3	#4	#5	#6	#7
Gender	male	female	female	female	male	male	female
Age at surgery (y)	57	74	58	75	68	54	83
Diagnosis	NSCLC	NSCLC	NSCLC	NSCLC	NSCLC	NSCLC	NSCLC
Histology	ADC	ADC	ADC	ADC	SCC	LCNEM	ADC
Localization	superior lobe left	superior lobe left, lingula	superior lobe right	lower lobe left	superior lobe right	superior lobe left	lower lobe left
Postop TNM	pT3 N1 M0	pT2a N0 M0	pT3 pN1 M0	pT2b N0 M0	pT1a N0 M0	pT2a N0 M0	pT2a N0 M0
Stage	IIIA	IB	IIIA	IIA	IA	IB	IB
Grade	G3	G2	G2	G2	G2	G3	G2
Smoking history (py)	60	n.e.	10	n.e.	n.e.	20	no
NACT	no	no	no	no	no	no	no

Abbreviations: NSCLC, non-small cell lung cancer; ADC, adenocarcinoma; SCC, squamous cell carcinoma; LCNEM, large-cell carcinoma with neuroendocrine morphology; n.e., not evaluable; py, pack years; Postop TNM, Post Operation TNM UICC 2009 classification (7th Edition); NACT, neoadjuvant chemo-therapy.

4.2 Variability in size

The size of the fragments was measured at the end of the experiment. Fragment size may influence the availability of nutrients and the elimination of waste products. The fragments are supplied with glucose, glutamine, and other essential nutrients only by diffusion. To guarantee an adequate supply, we aimed to cut the fragments of a size of approximately 1-2 mm diameter. The analysis of fragment size was focused on samples from two patients (#1 and #2), which all were cultured under starvation conditions, as illustrated in Figure 3. The smallest and the largest diameter of 30 fragments were measured with an inverse light optical microscope. The fragment sizes ranged from 0.6 mm to 2.79 mm. A statistically significant

difference was found between lung and tumour fragments sizes (smallest and largest diameter). As shown in Figure 3, lung fragments were on average larger compared with tumour fragments.

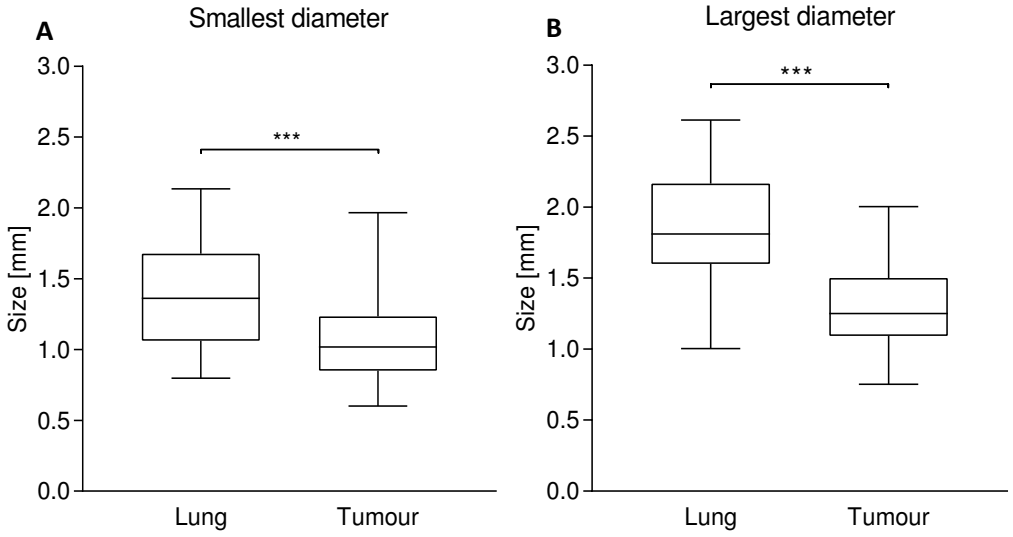

Figure 3 **| Size of lung and tumour fragments**. The box plot displays the size of fragments derived from lung or tumour tissue (n=30) 72 hours after starting the experiment (patients #1 and #2). (**A**) Smallest measured diameter of 30 fragments. (**B**) Largest measured diameter of 30 fragments. The lines show median, interquartile range, and the minimal to maximal range (whiskers). Group differences between lung and tumour tissues were assessed by Mann-Whitney-U-test. ***$p < 0.001$.

4.3 Heterogenous viability

In 3D models, like our organoid (fragment) model, tissue viability is of critical importance. Especially under the low glucose concentration in the media under starvation condition (1 mM) viability might be reduced. Thus, it was important to measure the fragments' viability, in a time-course experiment, as illustrated in Figure 4. A MTS assay was used to assess the viability of the lung and tumour samples. The measurements of patients #4, #5 (tumour excluded), #6 and #7 were performed at 0, 24, 48, and 72 hours after beginning of the treatment. Figure 4 demonstrates the variable chronical course of the viability of both lung and tumour, but not significant decrease over time. The weight-corrected OD at 24, 48, and 72 hours, were not statistically significant compared to the value at 0 hours.

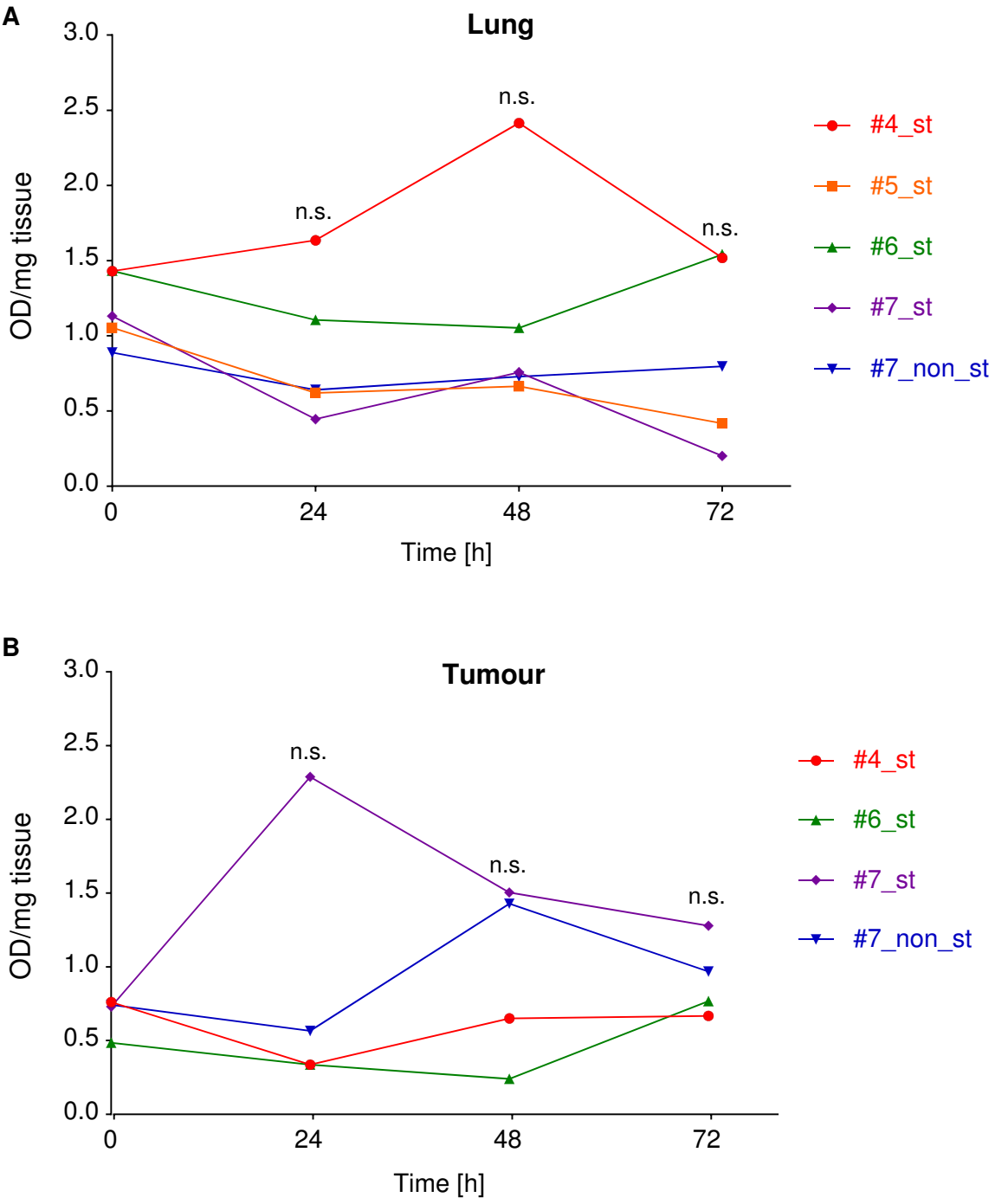

Figure 4 **| Viability of lung and tumour fragments.** Viability of fragments cultured *ex vivo* was measured by MTT test. OD (optical density) was measured for (**A**) lung (n=5) and (**B**) tumour tissues (n=4) at 0, 24, 48 and 72 hours after initiation of treatment. A negative control with fragments, killed with ethanol, was used. OD values were normalized to weight of each fragment. Approximately six fragments were measured per sample and condition. Fragments < 0.2 mg were excluded from analysis. Sample number and medium conditions are indicated in respective colours (# patient number_conditions; st, starvation; non_st, non-starvation). Tumour #5 was later excluded from analysis, since histological examination showed that the sample consisted primarily of lymph node. Group differences were calculated using One-Way ANOVA and Tukey´s HSD Post hoc test. n.s., not significant.

4.4 Microscopic changes of tumour and lung tissues

Cell death and necrosis are typical for larger solid tumours and *ex vivo* incubation might enhance cell death and lead to altered morphology. To analyse the viability and morphological appearance, HE stains of fresh untreated lung and tumour tissues (directly after lobectomy), as well as lung and tumour fragments after 72 hours of culture, were compared. The fresh lung slides looked normal according to the evaluation by a thoracic pathologist (PD Dr. Elvira Stacher-Priehse), despite occasionally destroyed alveolar structures. Fresh tumour tissues contained tumour cells, stroma tissue, lymphocyte infiltrates and necrosis in a variable manner. All fragments, both lung and tumour, showed decreased viability and signs of cell death, compared to the corresponding fresh tissues after 72 hours of culture. Lung fragments showed a moderate destruction of their alveolar structures. Tumour fragments exhibited a variable degree of necrotic changes, but no sample was totally necrotic. Figure 5 and 6 shows representative pictures of fresh lung and tumour tissue, as well as lung and tumour fragments under non-starvation (5 mM glucose with 10% dialyzed serum) and under starvation conditions (1 mM glucose and 0% dialyzed serum).

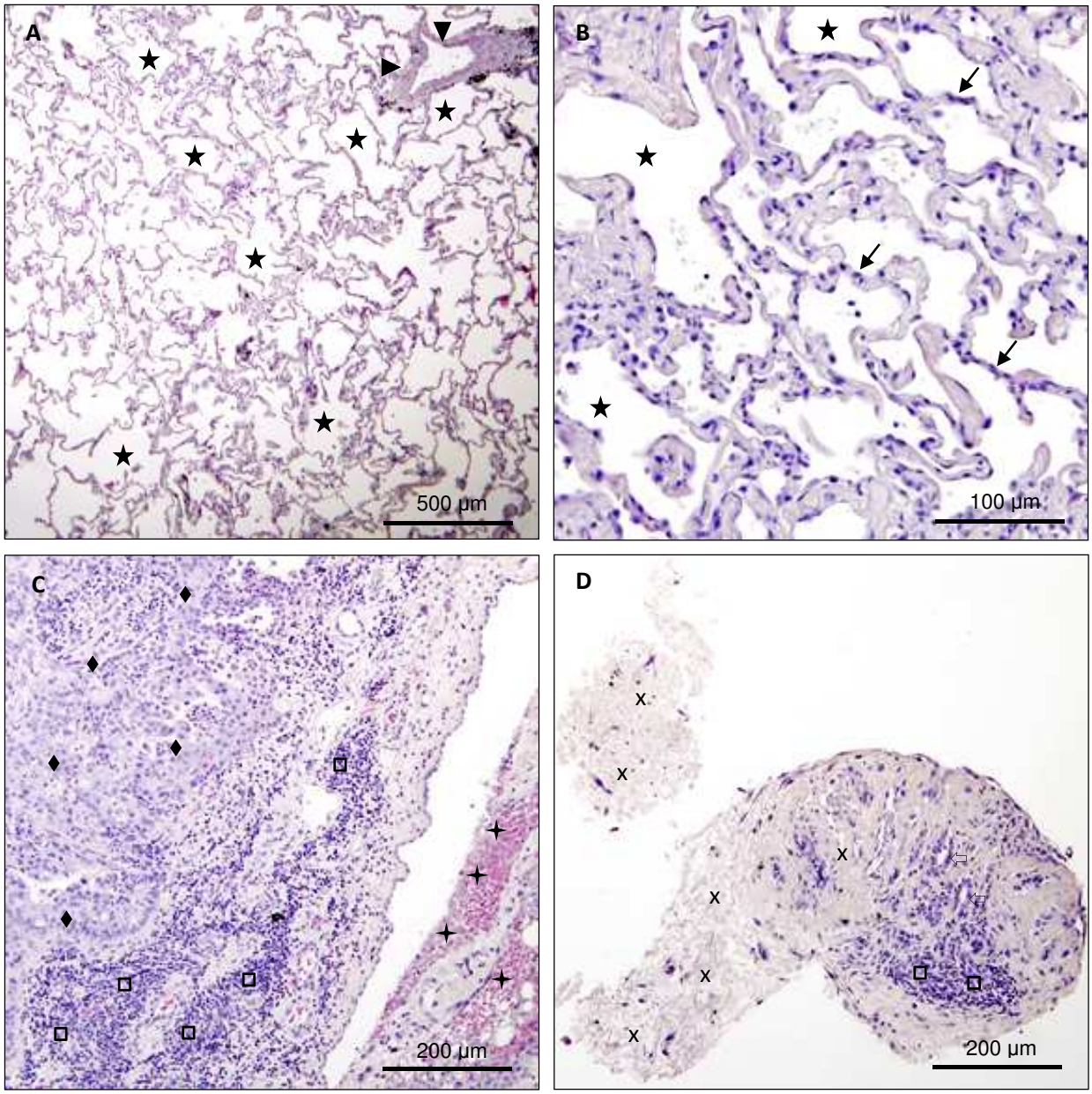

Figure 5 **| Representative fresh lung and tumour tissue fragments cultured under non-starvation conditions.** HE stains of (**A**) fresh lung tissue (patient #1) shows physiological alveolar structures with minimally fibrosed septa. (**B**) The lung fragment (patient #1) shows a similar structure after 72 hours of culture. (**C**) Fresh tumour tissue (patient #2, ADC) with papillary and tubular tumour structures. Tumour cells with considerably enlarged nuclei next to stroma tissue with many lymphocytes and characteristic necrosis. (**D**) Tumour fragment (patient #2, ADC) with gland formation ⇦ (oval lumen, lined by malignant columnar cells) after 72 hours of treatment. High proportion of stroma tissue and several lymphocytes. Representative HE stained sections are shown.★, alveolus ►, blood vessel; ↙, pneumocytes; ♦, tumour cells; ☐, lymphocytes; ✦, necrosis; ✕, stroma tissue; ADC, adenocarcinoma.

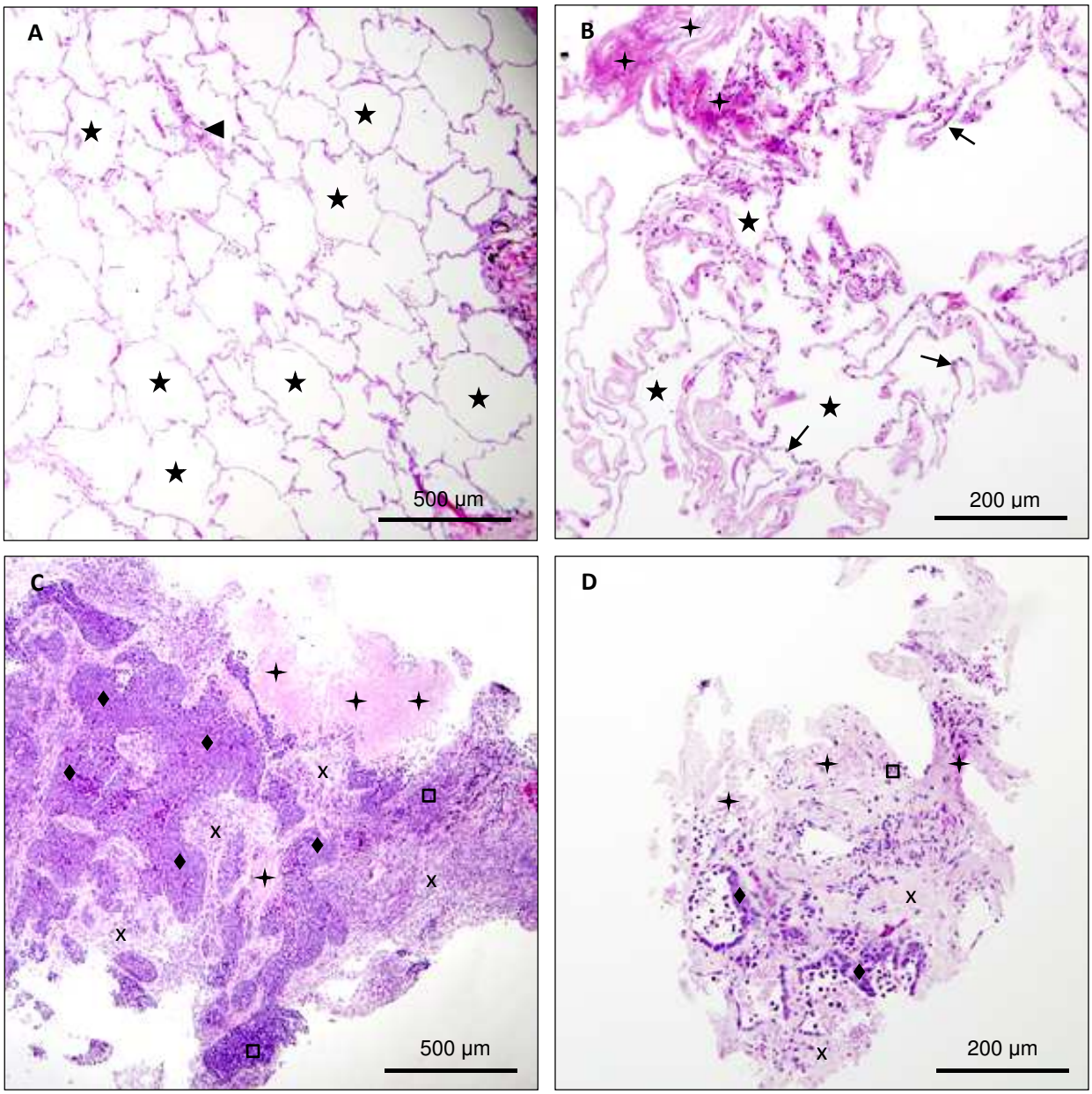

Figure 6 **| Representative fresh lung and tumour tissues as well as fragments cultured under starvation conditions.** HE stains of fresh lung (**A**) and tumour (**C**) tissue directly after lobectomy without treatment. A part of the fresh tissues was fragmented and cultured for 72 hours under starvation conditions. Then preparation of HE sections of lung (**B**) and tumour (D) fragments. (**A**) Fresh lung tissue (patient #7) presents physiological alveolar structures and blood vessels. (**B**) The lung fragment (patient #7) shows alveoli, stroma tissue and pneumocytes with decreased viability after 72 hours of treatment. A beginning necrosis is visible. (**C**) Fresh tumour tissue (patient #6, (LCNEM) with a high proportion of tumour cells and adjacent stroma tissue. Lymphocyte infiltration, mitoses and necrosis are typical. (**D**) Tumour fragment (patient #6, LCNEM) with tumour cell nests after 72 hours of culture. Abundant stroma tissue, several lymphocytes, and areas of necrosis. ★, alveolus; ►, blood vessel; ↙, pneumocytes; ♦, tumour cells; ☐, lymphocytes; ✦, necrosis; +, stroma tissue. LCNEM, large-cell carcinoma with neuroendocrine morphology.

4.5 Stable isotope labelling of glycerol in phospholipids

Glucose is one of the most important nutrients in cytoplasma (20). Normal and carcinoma cells use glucose, amongst other nutrients, to generate the glycerol backbone of new phospholipids via glycolysis. This pathway was detected in cell lines, but so far not in short time cultured lung and NSCLS fragments. In addition to this main route, under high starvation conditions cancer cell lines may potentially metabolise glutamine via the glyceroneogenesis pathway to generate G3P as a precursor for the phospholipid backbone. The key enzyme for this pathway, PCK2, has been shown to be expressed in lung cancer cells (39).

In order to analyse, whether the metabolic pathway to glycerol backbone synthesis can be measured using stable isotopes in the fragment model, lung and tumour fragments were cultured 72 hours in isotope labelled ($^{13}C_6$ glucose or $^{13}C_5$ glutamine) media. Both, non-starvation media containing physiological glucose (5 mM) and 10% dialyzed serum, and starvation media containing low glucose (1 mM) without serum were tested. The target variable was the percentage of stable isotope labelled carbon-skeleton of glycerol incorporated into phospholipids, after 72 hours of incubation with $^{13}C_6$ labelled glucose under starvation and non-starvation conditions. The metabolic pathways for the conversion of glucose or glutamine to glycerol are shown in Figure 7. Uniformly labelled glucose is metabolised via glycolysis into two molecules DHAP and into G3P (34).

Table 7 shows the phospholipid ion fragments (PC, PE, and PI), containing or not containing glycerol, with information about the molecular formula, chemical structure, and measured *m/z* via MS by Alexander Triebl, PhD (49). Our focus of interest in this analysis was the carbon-skeleton of glycerol. It was investigated how many (zero, one, two, three or four) labelled carbon atoms, derived from glucose or glutamine, were incorporated into the glycerol moiety of the phospholipid head group fragment ions.

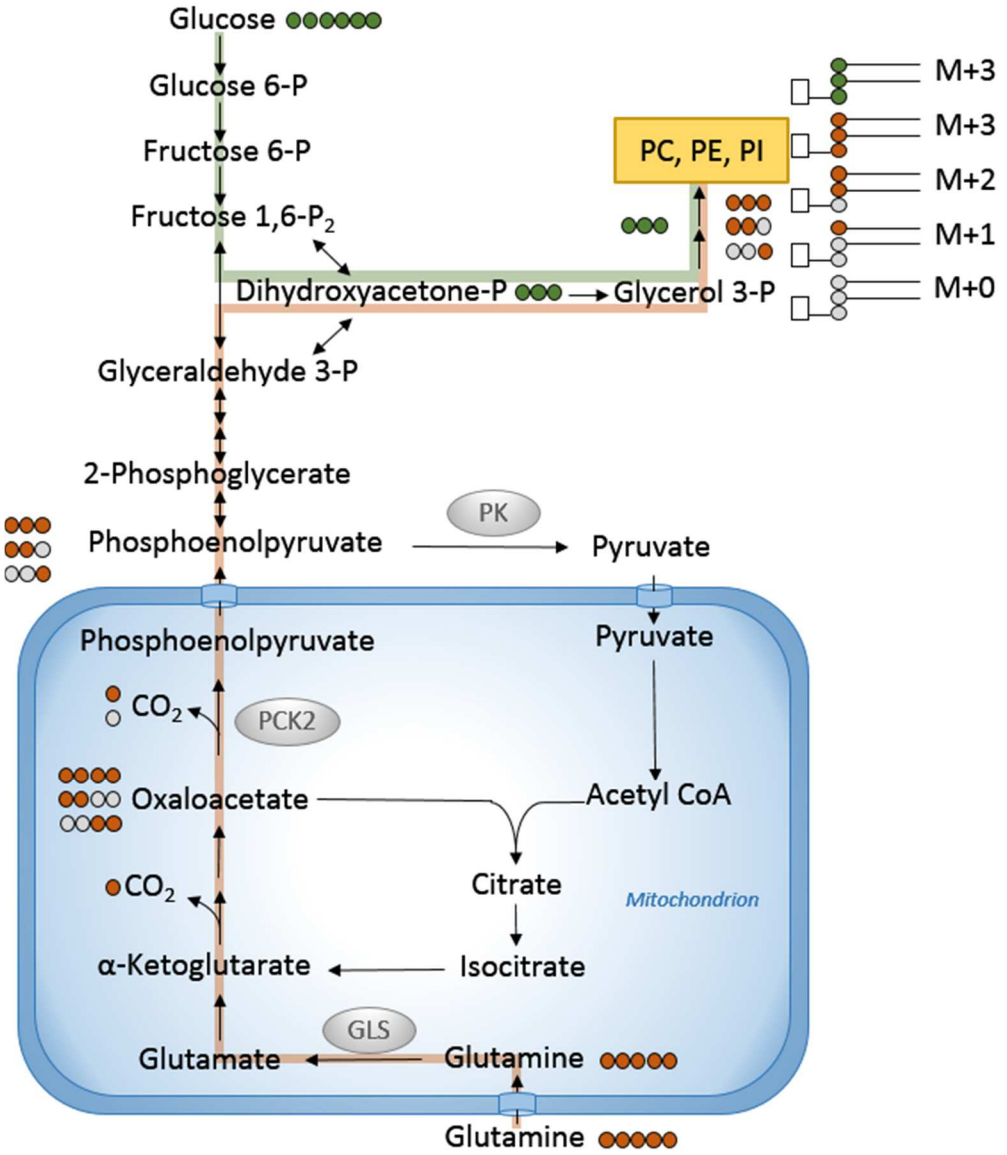

Figure 7 | **Metabolic pathway of uniformly labelled glucose via glycolysis, and glutamine via glyceroneogenesis, to generate the backbone of phospholipids**. Uniformly labelled glucose (six green dots corresponding to ^{13}C) is metabolised via glycolysis (highlighted in green) into two molecules dihydroxyacetone phosphate (molecule with three carbons). Dihydroxyacetone phosphate is reduced to glycerol 3-phosphate. Consequently, if glucose is the carbon source for glycerol 3-phosphate, glycerol backbones of PC, PE and PI incorporate three labelled carbons (three green dots) and show a mass number of M+3. Uniformly labelled glutamine (five orange dots corresponding to ^{13}C, pathway highlighted in orange) enters the mitochondrion through transporters, and is metabolised via glutamate (by glutaminase) and α-ketoglutarate into oxaloacetate (four orange dots). Now there are two ways: first, oxaloacetate enters a second turn in the TCA cycle forming oxaloacetate with two labelled carbons. Alternatively, as a second pathway, oxaloacetate is directly converted by PCK2 to phosphoenolpyruvate and CO_2. Phosphoenolpyruvate leaves the mitochondrion and is converted via glyceroneogenic pathway to glycerol 3-phosphate. Also, partially labelled oxaloacetate may enter the second pathway. Thus, there are three potential labelling patterns in the glycerol backbones of PC, PE, and PI if labelled glutamine is used as a carbon source: M+1, M+2 or M+3 (glycerol containing one, two, or three labelled carbons, respectively). If no labelled carbon is used (grey dots), there will be a mass number of M+0 in MS. GLS, glutaminase; P, phosphate; PC, phosphatidylcholine; PCK2, phosphoenolpyruvate carboxykinase 2 (mitochondrial isoform); PE, phosphatidylethanolamine; PI, phosphatidylinositol; PK, pyruvate kinase.

Carbons from $^{13}C_6$ labelled glucose were detected via MS in each phospholipid fragment head group (PC, PE, and PI) under non-starvation (Table 3) and starvation conditions (Table 4), as shown in Figures 8 and 9, right panel. The glycolysis pathway generates glycerol phosphate with three labelled atoms. Accordingly, the phospholipid head group fragment ions containing glycerol possessed a mass of M+0 (unlabelled form) or M+3 (with three labelled carbon atoms), while no M+1 or M+2 were found (Figures 8 and 9). In all phospholipid classes, ^{13}C enrichment from $^{13}C_6$ glucose was not significantly different in lung and tumour fragments. In tumour fragment under non-starvation conditions about one third of PC-glycerol and one third of PI-glycerol were fully labelled. PE showed the lowest transfer with about 20% labelling. In tumours under starvation conditions, $^{13}C_6$ glucose was incorporated into the glycerol backbone in about 15% of all PC phospholipids and in about 10% of all PE and PI. There were no significant differences in the glycerol label enrichments between lungs and tumours. In none of all seven tissue samples any conversion of uniformly labelled glutamine into PC, PE and PI-glycerol was measured, neither under starvation, nor under non-starvation conditions. In lung or tumour fragments cultured in media with unlabelled glucose only a low, normal background peak was measured, (data not shown). As a control, MS fragment ions lacking glycerol were measured. The glycerol-free fragment ions did not contain any ^{13}C label (Figures 8 and 9, left). All data were corrected for natural abundance.

Table 7 | **Overview of phospholipid head group fragment ions.**

Structure of phospholipid fragments	Molecular formula	Nominal *m/z*	Mass number
PC 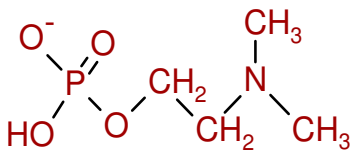	$C_4H_{11}O_4PN$	168	M+0
		169	M+1
		170	M+2
		171	M+3
PC + glycerol 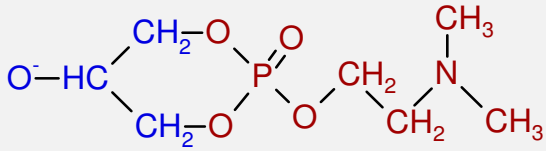	$C_7H_{15}O_5PN$	224	M+0
		225	M+1
		226	M+2
		227	M+3
PE 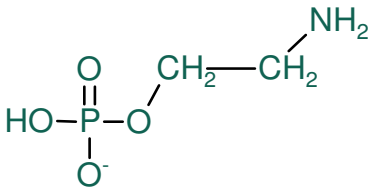	$C_2H_7O_4PN$	140	M+0
		141	M+1
		142	M+2
		143	M+3
PE frag + glycerol 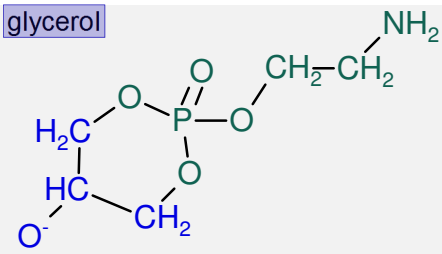	$C_5H_{11}O_5PN$	196	M+0
		197	M+1
		198	M+2
		199	M+3
PI frag 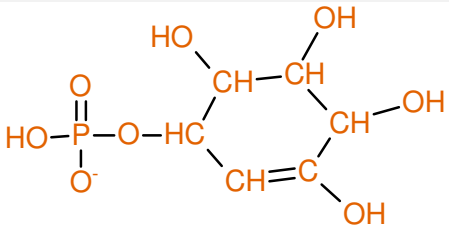	$C_6H_{10}O_8P$	241	M+0
		242	M+1
		243	M+2
		244	M+3
PI frag + glycerol 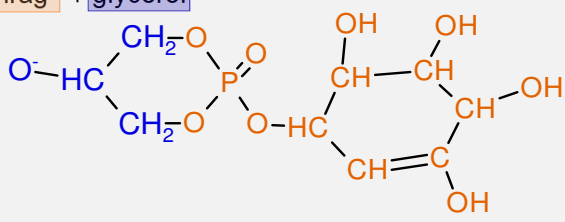	$C_9H_{14}O_9P$	297	M+0
		298	M+1
		299	M+2
		300	M+3

Abbreviations: PC, phosphatidylcholine; PE, phosphatidylethanolamine; PI, phosphatidylinositol; frag, fragment; +, containing. Data adapted with permission by Alexander Triebl, PhD (49).

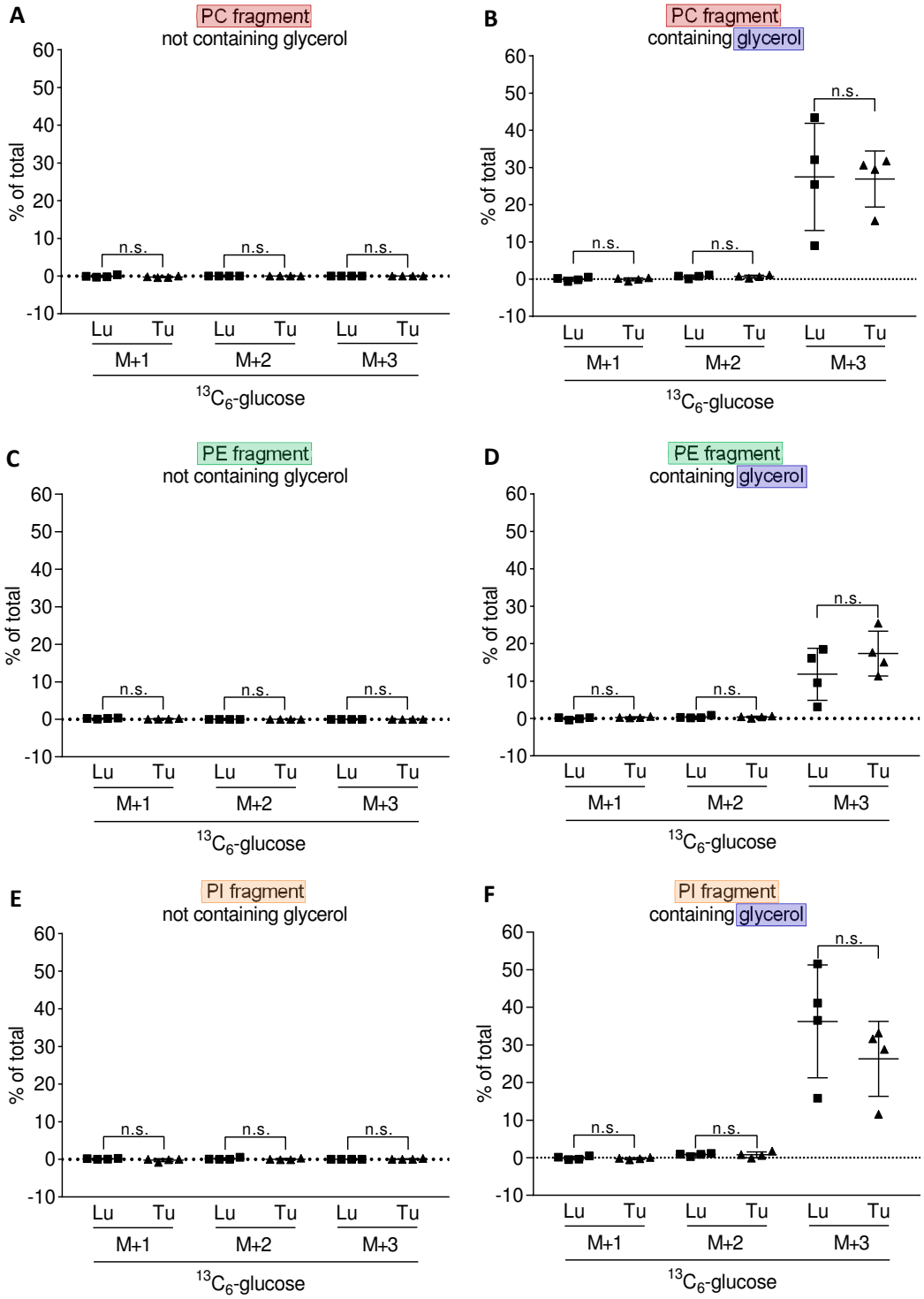

Figure 8 | **Results of MS analysis of phospholipid head group fragment ions under non-starvation conditions.** Samples from four patients (#1, #2, #3 and #7) were cultured in medium containing 5 mM fully ^{13}C-labelled glucose. The conversion of glucose into phospholipid head group fragment ions (PC, PE and PI) with or without glycerol was measured after 72 hours of treatment. Data of fragments with mass values M+0, M+1, M+2, M+3 and M+4 (not shown) were corrected for natural abundance. (**A**) MS results of phosphatidylcholine (PC) fragment isotopologues not containing glycerol (control). M+1, M+2 and M+3 denote fragments with one, two, or three labelled carbon atoms, respectively. (**B**) MS results of phosphatidylcholine (PC) fragment isotopologues containing glycerol from the same samples as in (**A**). (**C**),(**D**) MS results of phosphatidylethanolamine (PE) fragments not containing (**C**) or containing (**D**) glycerol. (**E**),(**F**) MS results of phosphatidylinositol (PI) not containing (**E**) or containing (**F**) glycerol. Group differences were calculated using Student´s t-test. n.s., not significant. * $p < 0.05$. Lu, lung; Tu, tumour.

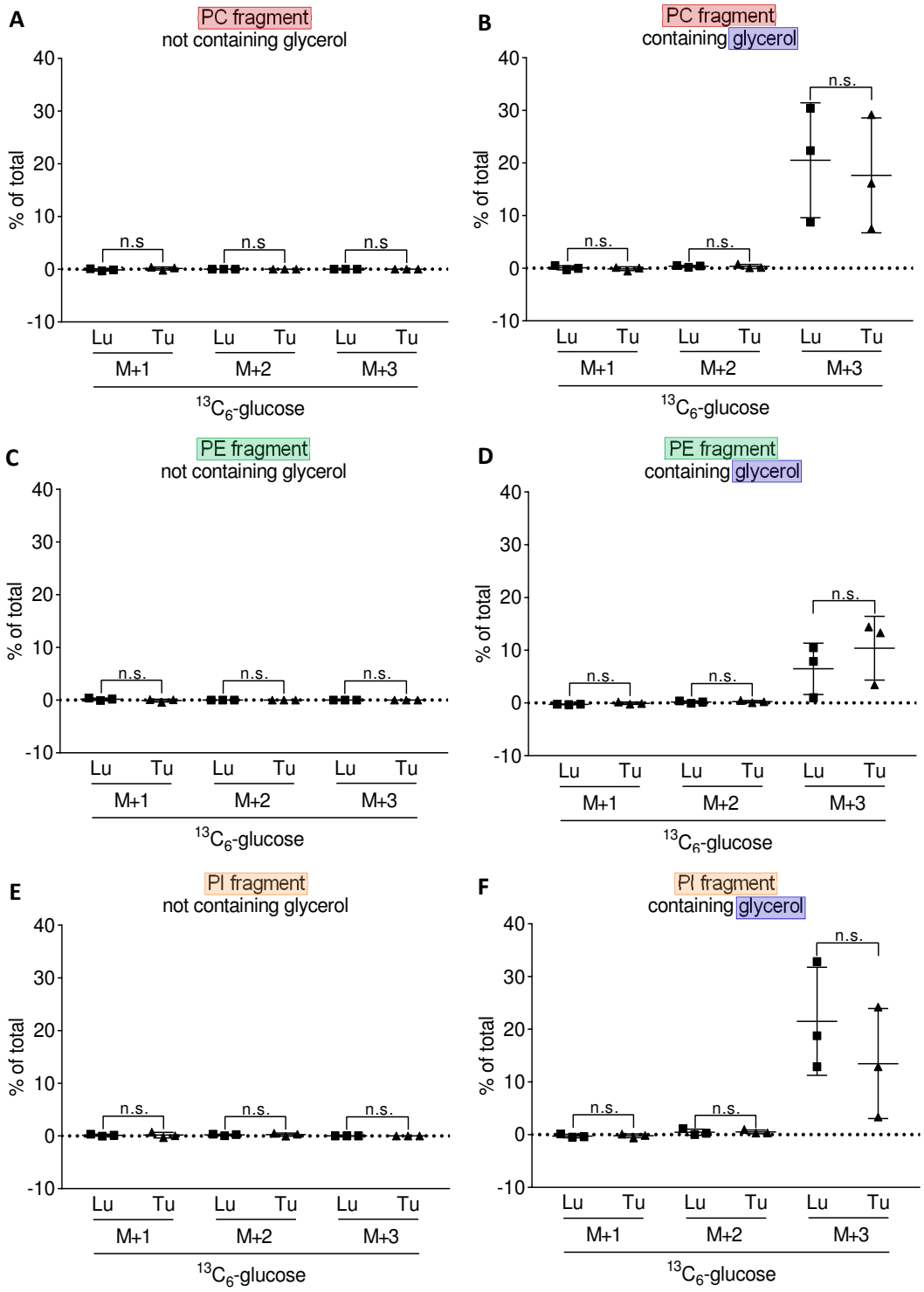

Figure 9 | **Results of MS analysis of different phospholipid classes under starvation conditions.** Samples of three patients (#4, #6, and #7) were cultured in medium containing 1 mM uniformly ^{13}C-labelled glucose. The conversion of glucose into phospholipid head group fragment ions (PC, PE and PI) with or without glycerol was measured after 72 hours of treatment. Data of fragments with mass values M+0, M+1, M+2, M+3 and M+4 were corrected for natural abundance. (**A**) Uptake of phosphatidylcholine (PC) not containing glycerol (control). M+1, M+2 and M+3 stand for isotopologues with one, two, or three labelled carbon atoms, respectively. (**B**) MS results of the same samples as in (**A**), but phosphatidylcholine (PC) fragment isotopologues containing glycerol. (**C**),(**D**) MS results of phosphatidylethanolamine (PE) not containing (**C**) glycerol or containing (**D**) glycerol. (**E**),(**F**) MS results of phosphatidylinositol (PI) not containing (**E**) glycerol or containing (**F**) glycerol. Group differences were calculated using Student´s t-test. n.s., not significant. *p < 0.05. Lu, lung; Tu, tumour.

5 Discussion

Investigations on cancer cell lines are usually the first step in cancer research, but they do not reflect the microenvironment of cancer completely. Metabolic pathways are intensively influenced by microenvironmental conditions, so that other model systems for studying cancer metabolism must be established. Tracer experiments with organoids could be an approach to investigate, how metabolites, like glucose or glutamine, are utilized in cancer tissue. The attention should be focused on cell products like phospholipids that are crucial for cell proliferation.

One aim of this study was to analyse, whether the metabolic pathway from glucose to the glycerol backbone of phospholipids can be studied in fresh human lung and NSCLC fragments (organoids) using isotope labelled tracers. The NSCLC and lung tissues were obtained from previously untreated lung cancer patients and cultured *ex vivo*. Some other research groups applied intravenously stabile isotope labelled metabolomics in NSCLC patients prior to surgical resection. Later on, they analysed liquid N_2 frozen tissue slices by MS (30, 56). However, these results are probably influenced by systemic metabolism and regulations, e.g. by the liver. In contrast, in our study tissue fragments were cultured in media with uniformly labelled $^{13}C_6$ glucose or $^{13}C_5$ glutamine, under physiological conditions and mild starvation conditions mimicking the cancer microenvironment. The test procedure included analysis of clinical data, fragment sizes, tissue viability and histological quality. Metabolic activity in respect to phospholipid biosynthesis was analysed using stable isotope labelled tracers (glucose and glutamine). The primary aim of our study was to investigate the feasibility and limitations of this model. As a second aim, the possible use of glutamine as alternative carbon source for glycerol synthesis via glyceroneogenesis was investigated.

5.1 Feasibility and limitations of the *ex vivo* model

Both, lung cancer and lung tissue were suitable for dissection into small fragments. Daily medium change could be performed easily without disrupting the tissue. Tissue preparation for MS included mechanical disruption by a tissue homogenizer (“Ultraturrax”) followed by sonication. This procedure yielded tissue homogenates that were suitable for analysis. MTS assay showed a variable chronical course, but

no clear tendency to reduction of cell viability over time. These results indicated that an active cell metabolism existed throughout the experiment. It is important to note that the tissue fragments consisted of different cell types, tumour cells, stroma cells, and other cells (e.g. lymphocytes or macrophages). Thus, this model reflects the interplay of different cell types in tumours *in vivo*.

The MS analysis was performed by Alexander Triebl, PhD, who established a method to analyse the isotopologues of glycerol bound to phospholipids in cells (Leithner et al, manuscript in preparation). In this study we showed that this method can also be applied to study tissue fragments cultured *ex vivo*. In tumour and lung fragments cultured in $^{13}C_6$ glucose, a conversion of glucose to the glycerol backbone was measured by MS in all three phospholipid groups (PC, PE and PI). The observed variation of the measurement values could be attributable to inter-patient differences. The utilisation of stable isotope labelled glucose for the analysis of lipid synthesis in an *ex vivo* cancer model has not been not described in the literature so far, to the best of our knowledge.

Lung and tumour differed significantly in their fragments size. Tumour fragments were significantly smaller than lung fragments. Difference in size could be due to the spongy and heterogeneous consistency of tumour tissue, which complicated the fragmentation in equal-sized pieces. Possibly also, the tumour fragments were influenced by necrotic changes. Since two different persons were involved in fragmenting the tissue, in order to avoid a delay in the processing of the tissue, a possible person-related difference cannot be excluded. Since fragment size may possibly influence the viability and the supply with nutrients, it is important to achieve similar fragment size in future studies. The preparation of HE stains turned out to be extraordinarily important to assess the histological viability of fragments. In addition, examination of HE stained sections of tumour patient #5 identified the tissue as lymph node. Thus, patient #5 was excluded from further analysis. After 72 hours of culture, cell death and decrease of viability were visible by morphological examination. Samples cultured under starvation conditions (medium with 1 mM glucose without serum) showed more necrotic changes than samples cultured under physiological conditions (medium with 5 mM glucose and 10% dialyzed serum). Tissue viability is a critical point for all *ex vivo* studies, including metabolic

studies. Shorter time of culture, for example eight or twelve hours instead of 72 hours, might positively affect the viability. On the other hand, such a short incubation time might result in a very low enrichment values for ^{13}C in a metabolic end product, like phospholipids. Lane et al. (35) showed that the synthesis of the glycerol backbone of phospholipids from glucose is detectable after six hours. In general, it is recommended to achieve a metabolic and isotopic steady state in isotope label experiments: the concentration of target parameter and enrichment of stable isotopic tracer must reach a plateau (glycolysis in minutes, TCA after several hours). This process depends on flux from nutrient to metabolite and on pool size (57). However, to achieve isotopic steady state might be difficult or impossible in the case of phospholipids, which have comparatively large pool size. The subsidence of fragments on the ground of the well-plate is caused by gravity. Consequently, supply with nutrients from the medium could be restricted. A useful modification of the experiment set-up would be to rock or shake the well-plates all the time.

5.2 Conversion of uniformly labelled glucose and glutamine

The novel fragment model was further utilized to study the conversion of glucose or glutamine into the glycerol backbone of phospholipids. The percentage of stable isotope labelled glycerophospholipid backbones were analysed by MS in cooperation with Alexander Triebl, PhD Core Facility Mass Spectrometry and Lipidomics (CMR), Medical University of Graz. Tissue fragments incubated with unlabelled glucose or glutamine were used as a control. The *ex vivo* model was applied under physiological and nutrient-poor, cancer-like conditions.

In tissue fragments derived from all seven patients cultured with $^{13}C_6$ labelled glucose, uptake conversion to the glycerol backbone of phospholipids was detected. The detected MS fragment ion isotopologues (M+3) corresponded to fully labelled glycerol within the phospholipid head group. Because of the enzymatic steps of glycolysis, there is only G3P with three labelled carbons that could be used for glycerol backbone synthesis. This result was observed for all three phospholipid groups (PC, PE and PI) under both, non-starvation and starvation conditions. The differences in the glycerol label enrichments between lung and tumour were not significant. However, the variability was quite high, and number of samples included

in our study was low. Thus, possible differences in phospholipid biosynthetic activities between lung and tumour tissue might have been not detected in our study.

Another working group, also led by Univ.-Ass. Priv.-Doz. Dr. med. univ. Katharina Leithner, PhD obtained research data in two lung cancer cell lines *in vitro* that suggest the use of glutamine for building glycerol backbone of phospholipids (glyceroneogenesis) under very low 0.2 mM glucose conditions in the media (Leithner et al, manuscript in preparation). Based on these results, the second objective of this pilot study was to examine, whether $^{13}C_5$ labelled glutamine was converted via the glyceroneogenesis pathway into the glycerol backbone in fresh NSCLC tissues. MS analysis of our fragments cultured in media (5 mM as well as 1 mM glucose) with $^{13}C_5$ glutamine detected no conversion to the phospholipid head group fragment ions. The conversion of glutamine in fragments *ex vivo* contrasts to the conduct in lung cancer cell lines *in vitro*. However, this conversion might be occurred only at very low glucose levels (0.2 mM in lung cancer cell lines), while in our fragment study we used 1 mM or 5 mM glucose in order to limit the loss of cell viability. So, cancer cells might switch their metabolism to glyceroneogensis only under a higher stress level. Possibly, at 1 mM glucose the fragments are only able to use less glucose to generate glycerol, but an alternative second metabolic pathway is not activated yet. Under our nutrient conditions, glutamine is not used via glyceroneogensis to generate the glycerol backbone of phospholipids. In cancer cells glutamine has been shown to be converted also into other metabolites, for example lactate or alanine (20). Thus, cell metabolism of cancer cell lines *in vitro* and cancer tissue *ex vivo* might differ.

5.3 Conclusion

The results of this study show, that the *ex vivo* fragment (organoid) NSCLC model is suitable for investigation of metabolic pathways using stable isotope labelled glucose. However, tissue and fragment heterogeneity and declining tissue viability are major limitations and should be improved. Future research projects should investigate how different fragments sizes influence the tissue viability. In addition, medium with lower glucose concentrations may stress fragments and force them to switch their metabolic pathways to ensure cell survival. A shorter time of incubation and modified culture conditions (rocking or shaking) might improve fragment viability. A further approach could be to analyse other metabolic pathways and other end-products that derived from glucose or glutamine. In summary, the test procedure was feasibly good in practice. This model is an ideal starting position for further investigations.

References

1. World Cancer Report 2014. Lyon: International Agency for Research on Cancer; 2014 [cited 24 October, 2017]. Available from: http://publications.iarc.fr/Non-Series-Publications/World-Cancer-Reports/World-Cancer-Report-2014.
2. Luftröhre, Bronchien und Lunge (C33-C34) - Krebsinzidenz (Neuerkrankungen pro Jahr), Österreich ab 1983 Vienna: STATISITK AUSTRIA; [updated 22 December 2016; cited 06 December 2017]. Available from: http://www.statistik.at/web_de/statistiken/menschen_und_gesellschaft/gesundheit/krebserkrankungen/luftroehre_bronchien_lunge/021766.html.
3. Luftröhre, Bronchien und Lunge (C33-C34) - Krebsmortalität (Sterbefälle pro Jahr), Österreich ab 1983 Vienna: STATISTIK AUSTRIA; [updated 22 December 2016; cited 06 December 2017]. Available from: http://www.statistik.at/web_de/statistiken/menschen_und_gesellschaft/gesundheit/krebserkrankungen/luftroehre_bronchien_lunge/021767.html.
4. Cagle PT, Allen TC, Dacic S, Kerr MK, Beasley MB. Advances in surgical pathology. Cagle PT, Timothy CA, editors. Philadelphia, PA: LWW; 2010. 11-24 p.
5. Travis WD, Brambilla E, Riely GJ. New pathologic classification of lung cancer: relevance for clinical practice and clinical trials. J Clin Oncol. 2013;31(8):992-1001.
6. Travis WD, Brambilla E, Nicholson AG, Yatabe Y, Austin JHM, Beasley MB, et al. The 2015 World Health Organization Classification of Lung Tumors: Impact of Genetic, Clinical and Radiologic Advances Since the 2004 Classification. Journal of Thoracic Oncology. 2015;10(9):1243-60.
7. Hou J, Aerts J, den Hamer B, van Ijcken W, den Bakker M, Riegman P, et al. Gene expression-based classification of non-small cell lung carcinomas and survival prediction. PLoS One. 2010;5(4):e10312.
8. Molina JR, Ping Y, Cassivi SD, Schild SE, Adjei AA. Non-Small Cell Lung Cancer: Epidemiology, Risk Factors, Treatment, and Survivorship. Mayo Clinic Proceedings. 2008;83(5):584-94.
9. Sher T, Dy GK, Adjei AA. Small Cell Lung Cancer. Mayo Clinic Proceedings. 2008;83(3):355-67.
10. Lababede O, Meziane M, Rice T. Seventh edition of the cancer staging manual and stage grouping of lung cancer: quick reference chart and diagrams. Chest. 2011;139(1):183-9.
11. Silvestri GA, Gonzalez AV, Jantz MA, Margolis ML, Gould MK, Tanoue LT, et al. Methods for staging non-small cell lung cancer: Diagnosis and management of lung cancer, 3rd ed: American College of Chest Physicians evidence-based clinical practice guidelines. Chest. 2013;143(5 Suppl):e211S-50S.
12. Griesinger F, Eberhardt WE, Früh M, Gautschi O, Hilbe W, Hoffmann H, et al. Onkopedia Leitlinien, Solide Tumoren: Lungenkarzinom, nicht-kleinzellig (NSCLC) Vienna: Österreichische Gesellschaft für Hämatologie & Medizinische Onkologie; 2017 [updated April 2017; cited 05 December], 2017. Available from: http://www.oegho.at/onkopedia-leitlinien/solide-tumore/lungenkarzinom-nicht-kleinzellig-nsclc-copy-1.html.
13. Goldstraw P, Chansky K, Crowley J, Rami-Porta R, Asamura H, Eberhardt WE, et al. The IASLC Lung Cancer Staging Project: Proposals for Revision of the TNM Stage Groupings in the Forthcoming (Eighth) Edition of the TNM Classification for Lung Cancer. J Thorac Oncol. 2016;11(1):39-51.
14. Rami-Porta R, Bolejack V, Crowley J, Ball D, Kim J, Lyons G, et al. The IASLC Lung Cancer Staging Project: Proposals for the Revisions of the T Descriptors in the Forthcoming Eighth Edition of the TNM Classification for Lung Cancer. J Thorac Oncol. 2015;10(7):990-1003.
15. Bensinger SJ, Christofk HR. New aspects of the Warburg effect in cancer cell biology. Semin Cell Dev Biol. 2012;23(4):352-61.
16. Balkwill FR, Capasso M, Hagemann T. The tumor microenvironment at a glance. J Cell Sci. 2012;125(Pt 23):5591-6.

17. Birsoy K, Possemato R, Lorbeer FK, Bayraktar EC, Thiru P, Yucel B, et al. Metabolic determinants of cancer cell sensitivity to glucose limitation and biguanides. Nature. 2014;508(7494):108-12.
18. Cairns RA, Harris IS, Mak TW. Regulation of cancer cell metabolism. Nat Rev Cancer. 2011;11(2):85-95.
19. Montal Emily D, Dewi R, Bhalla K, Ou L, Hwang Bor J, Ropell Ashley E, et al. PEPCK Coordinates the Regulation of Central Carbon Metabolism to Promote Cancer Cell Growth. Molecular Cell.60(4):571-83.
20. DeBerardinis RJ, Mancuso A, Daikhin E, Nissim I, Yudkoff M, Wehrli S, et al. Beyond aerobic glycolysis: transformed cells can engage in glutamine metabolism that exceeds the requirement for protein and nucleotide synthesis. Proc Natl Acad Sci U S A. 2007;104(49):19345-50.
21. Fouad YA, Aanei C. Revisiting the hallmarks of cancer. American Journal of Cancer Research. 2017;7(5):1016-36.
22. Vander Heiden MG, Cantley LC, Thompson CB. Understanding the Warburg effect: the metabolic requirements of cell proliferation. Science. 2009;324(5930):1029-33.
23. Ackerman D, Simon MC. Hypoxia, lipids, and cancer: surviving the harsh tumor microenvironment. Trends Cell Biol. 2014;24(8):472-8.
24. Boroughs LK, DeBerardinis RJ. Metabolic pathways promoting cancer cell survival and growth. Nat Cell Biol. 2015;17(4):351-9.
25. Harris AL. Hypoxia - a key regulatory factor in tumour growth. Nat Rev Cancer. 2002;2(1):38-47.
26. Brown JM, Giaccia AJ. The unique physiology of solid tumors; opportunities (and problems) for cancer therapy. Cancer Res. 1998;58:1408-16.
27. Polet F, Feron O. Endothelial cell metabolism and tumour angiogenesis: glucose and glutamine as essential fuels and lactate as the driving force. J Intern Med. 2013;273(2):156-65.
28. Gatenby RA, Gillies RJ. Why do cancers have high aerobic glycolysis? Nat Rev Cancer. 2004;4(11):891-9.
29. Cheng TL, Sudderth J, Yang CD, Mullen AR, Jin ES, Mates JM, et al. Pyruvate carboxylase is required for glutamine-independent growth of tumor cells. P Natl Acad Sci USA. 2011;108(21):8674-9.
30. Sellers K, Fox MP, Bousamra M, 2nd, Slone SP, Higashi RM, Miller DM, et al. Pyruvate carboxylase is critical for non-small-cell lung cancer proliferation. J Clin Invest. 2015;125(2):687-98.
31. Kroemer G, Pouyssegur J. Tumor cell metabolism: cancer's Achilles' heel. Cancer Cell. 2008;13(6):472-82.
32. Vincent EE, Sergushichev A, Griss T, Gingras MC, Samborska B, Ntimbane T, et al. Mitochondrial Phosphoenolpyruvate Carboxykinase Regulates Metabolic Adaptation and Enables Glucose-Independent Tumor Growth. Mol Cell. 2015;60(2):195-207.
33. Yuneva MO, Fan TW, Allen TD, Higashi RM, Ferraris DV, Tsukamoto T, et al. The metabolic profile of tumors depends on both the responsible genetic lesion and tissue type. Cell Metab. 2012;15(2):157-70.
34. Berg JM, Tymoczko JL, Gatto GJ, Stryer L. Biochemistry. 8th ed. New York: W. H. Freeman & Co Ltd; 2015.
35. Lane AN, Fan TW, Xie Z, Moseley HN, Higashi RM. Isotopomer analysis of lipid biosynthesis by high resolution mass spectrometry and NMR. Anal Chim Acta. 2009;651(2):201-8.
36. Yuneva M, Zamboni N, Oefner P, Sachidanandam R, Lazebnik Y. Deficiency in glutamine but not glucose induces MYC-dependent apoptosis in human cells. J Cell Biol. 2007;178(1):93-105.
37. Altman BJ, Stine ZE, Dang CV. From Krebs to clinic: glutamine metabolism to cancer therapy. Nat Rev Cancer. 2016;16(10):619-34.
38. Yang J, Kalhan SC, Hanson RW. What is the metabolic role of phosphoenolpyruvate carboxykinase? J Biol Chem. 2009;284(40):27025-9.

39. Leithner K, Hrzenjak A, Trotzmuller M, Moustafa T, Kofeler HC, Wohlkoenig C, et al. PCK2 activation mediates an adaptive response to glucose depletion in lung cancer. Oncogene. 2015;34(8):1044-50.
40. Mendez-Lucas A, Hyrossova P, Novellasdemunt L, Vinals F, Perales JC. Mitochondrial phosphoenolpyruvate carboxykinase (PEPCK-M) is a pro-survival, endoplasmic reticulum (ER) stress response gene involved in tumor cell adaptation to nutrient availability. J Biol Chem. 2014;289(32):22090-102.
41. Bohdanowicz M, Grinstein S. Role of phospholipids in endocytosis, phagocytosis, and macropinocytosis. Physiol Rev. 2013;93(1):69-106.
42. Nadkarni RR, Abed S, Draper JS. Organoids as a model system for studying human lung development and disease. Biochemical and Biophysical Research Communications. 2016;473(3):675-82.
43. Hanahan D, Weinberg RA. Hallmarks of cancer: the next generation. Cell. 2011;144(5):646-74.
44. Fatehullah A, Tan SH, Barker N. Organoids as an in vitro model of human development and disease. Nat Cell Biol. 2016;18(3):246-54.
45. Schmid JO, Dong M, Haubeiss S, Friedel G, Bode S, Grabner A, et al. Cancer cells cue the p53 response of cancer-associated fibroblasts to cisplatin. Cancer Res. 2012;72(22):5824-32.
46. Fan TW, Lane AN, Higashi RM, Yan J. Stable isotope resolved metabolomics of lung cancer in a SCID mouse model. Metabolomics. 2011;7(2):257-69.
47. Sandra K, Sandra P. Lipidomics from an analytical perspective. Curr Opin Chem Biol. 2013;17(5):847-53.
48. Meyer VR. Practical High Performance Liquid Chromatography, Fourth edition. Fourth ed. United Kingdom: John Wiley & Sons, Ltd; 2004.
49. Triebl A. Sophisticated Analytical Methods for Lipidomics [dissertation]. Graz: Medical University of Graz; 2016.
50. Triebl A, Trotzmuller M, Eberl A, Hanel P, Hartler J, Kofeler HC. Quantitation of phosphatidic acid and lysophosphatidic acid molecular species using hydrophilic interaction liquid chromatography coupled to electrospray ionization high resolution mass spectrometry. J Chromatogr A. 2014;1347:104-10.
51. Gross JH. Massenspektrometrie. Berlin Heidelberg: Springer-Verlag; 2013.
52. van Grieken R, de Bruin M. Nomenclature for radioanalytical chemestry (IUPAC Recommendations 1994). Pure & Appl Chem. 1994;66(12):2516-26.
53. Calvert JG. Glossary of atmospheric chemistry terms (Recommendations 1990). Pure & Appl Chem. 1990;62(11):2167-219.
54. Müller P. Glossary of terms used on physical organic chemestry (IUPAC Recommendations 1994). Pure & Appl Chem. 1994;66(5):1077-184.
55. Coplen TB, Böhlke JK, De Briève P, Ding T, Holden NE, Hopple JA, et al. Isotope-abundance variations of selected elements (IUPAC Technical Report). Pure Appl Chem. 2002;74(10):1987-2017.
56. Lane AN, Fan TW, Bousamra M, 2nd, Higashi RM, Yan J, Miller DM. Stable isotope-resolved metabolomics (SIRM) in cancer research with clinical application to nonsmall cell lung cancer. OMICS. 2011;15(3):173-82.
57. Buescher JM, Antoniewicz MR, Boros LG, Burgess SC, Brunengraber H, Clish CB, et al. A roadmap for interpreting (13)C metabolite labeling patterns from cells. Curr Opin Biotechnol. 2015;34:189-201.